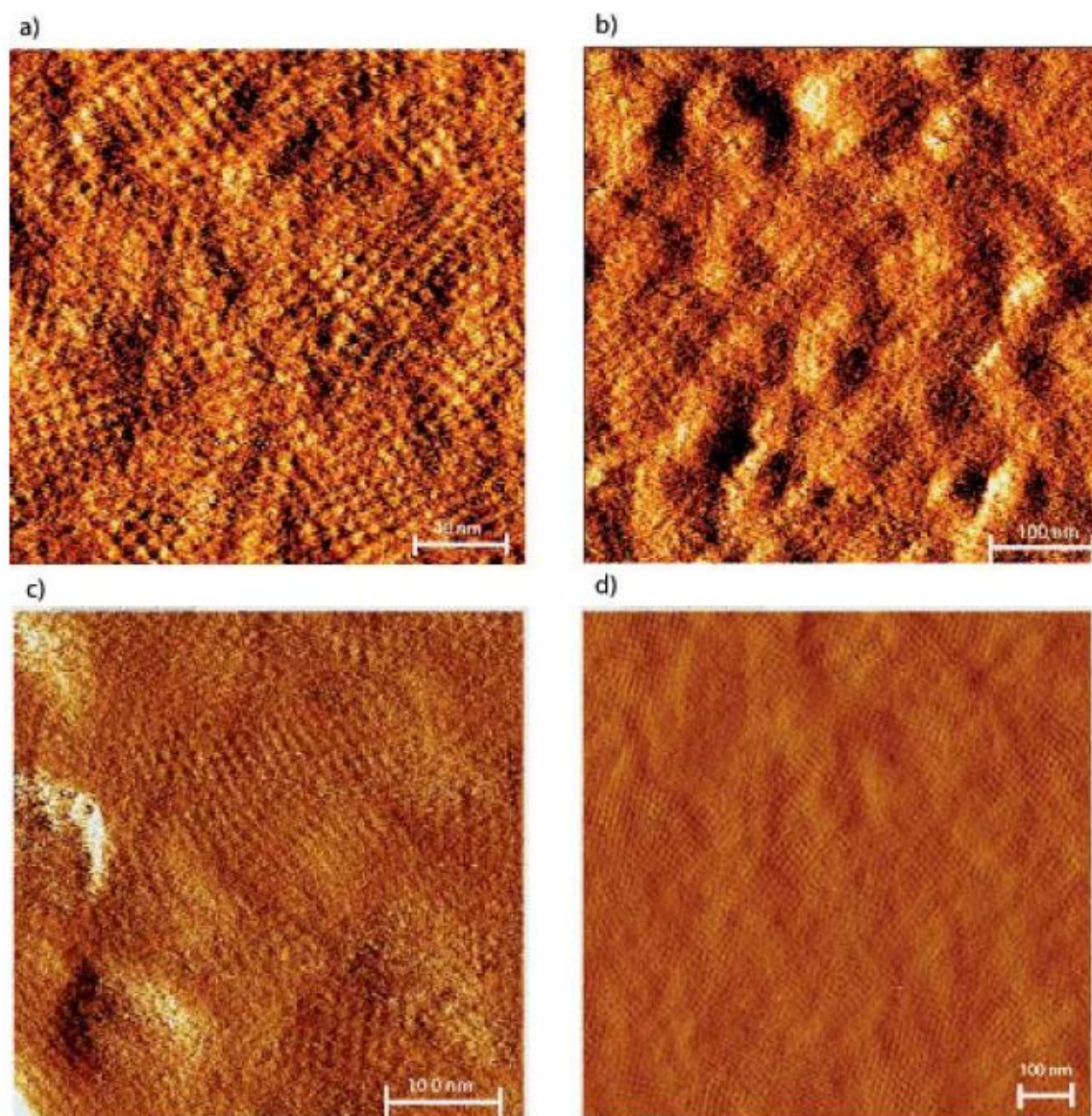
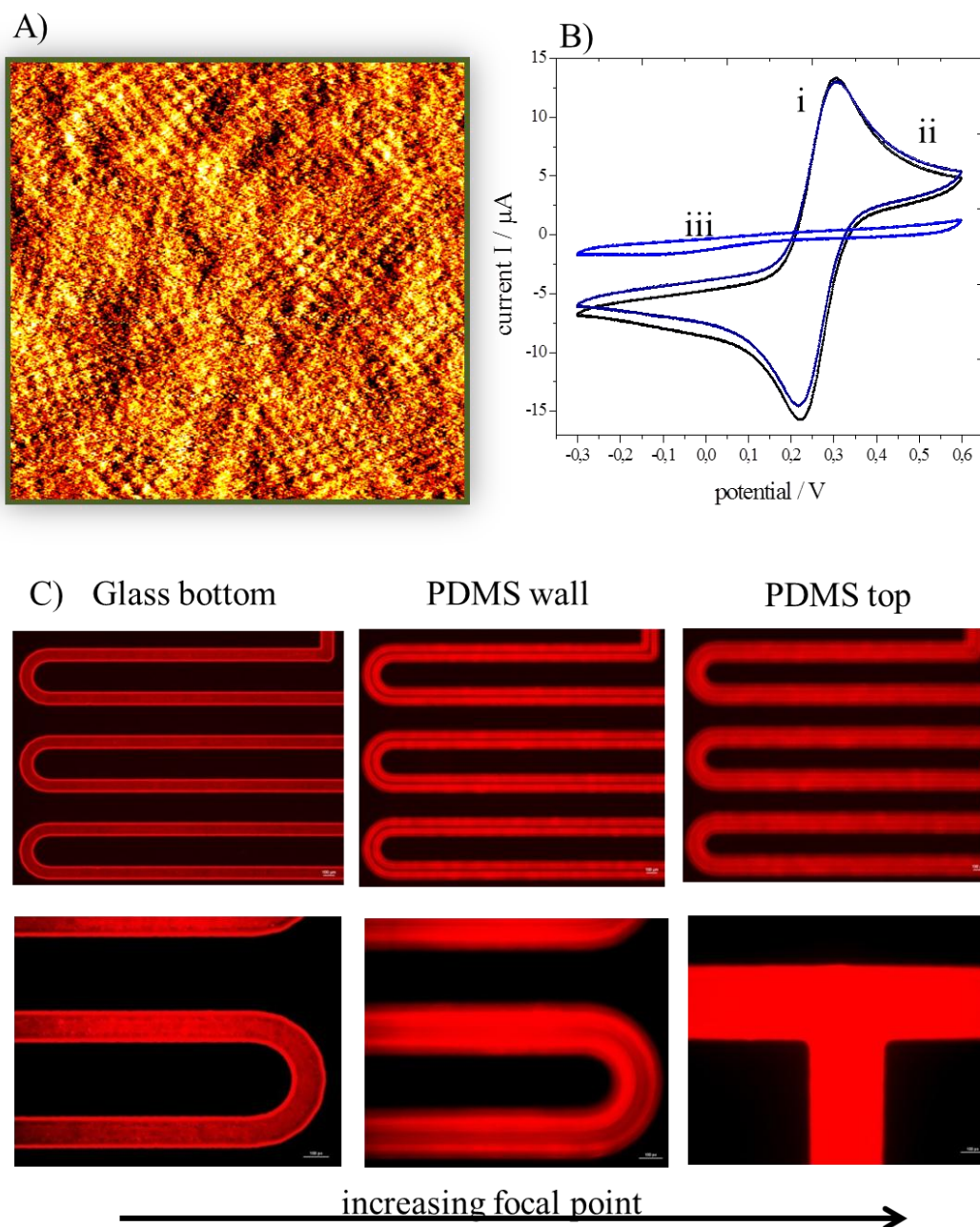


**Suppl. Fig. 1** Pictures of the LOC set up and microfluidic biochip consisting of four integrated microreactor each containing three electrode set up



**Suppl. Fig. 2:** AFM images of crystalline SbpA monolayers on a) gold, b) platinum, c) glass and d) PDMS.

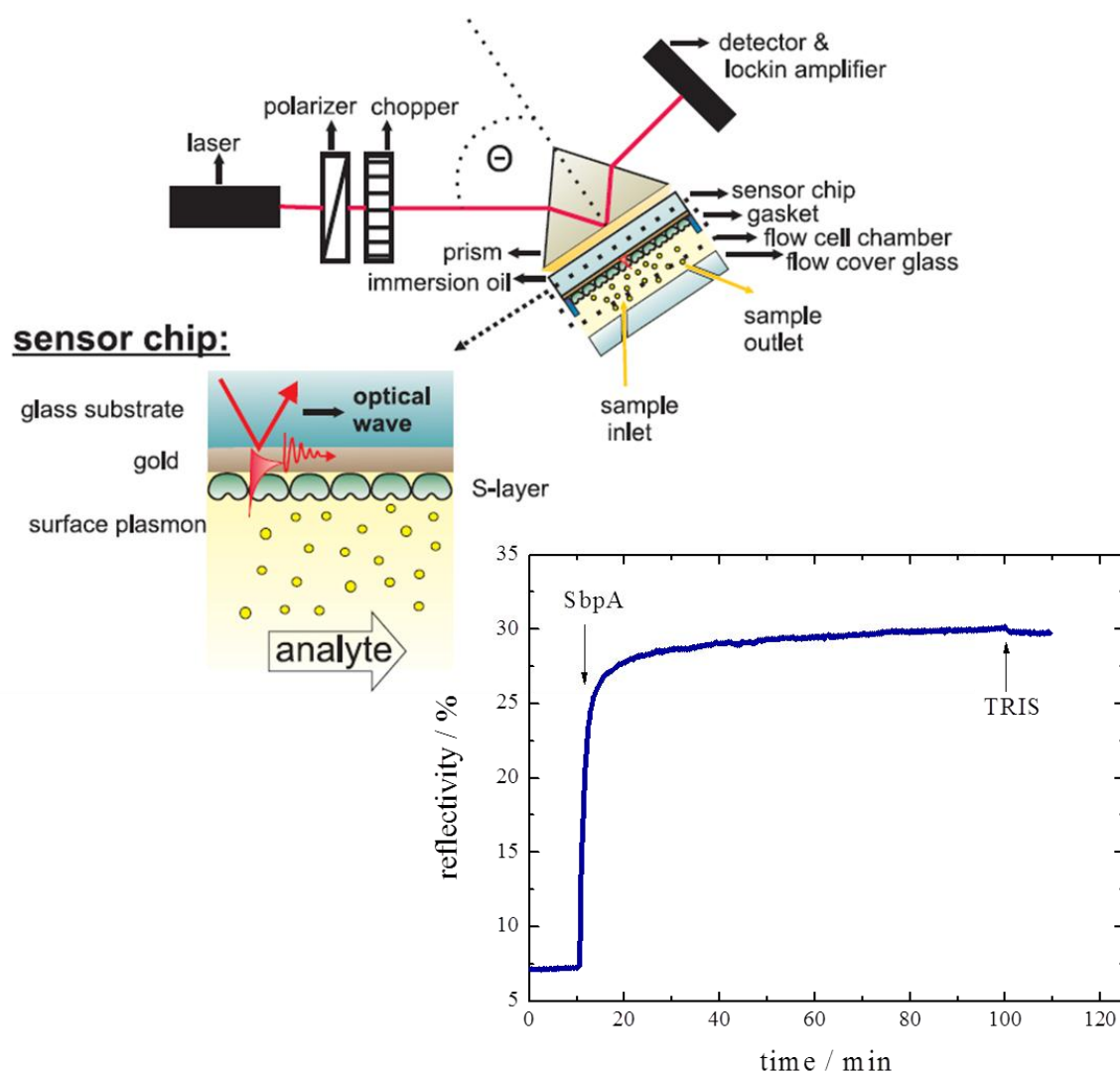
Atomic Force Microscopy (AFM) was applied to image the formation of S-layer lattices on PDMS, glass, gold and platinum. After extensive cleaning using isopropanol and DI water, the different microchip surfaces were covered with 200  $\mu$ L of SbpA protein solution (0.1 mg/mL in 0.5 mM TRIS and 10 mM  $\text{CaCl}_2$ , pH 9.0). Following overnight recrystallization at room temperature, the surfaces were rinsed with DI water and were placed into the atomic force microscope (AFM Nanoscope IIIa). After wetting the sample surface with 0.1 M NaCl solution, imaging was performed in liquid using contact mode. Oxide-sharpened silicon nitride cantilevers (NanoProbes, Digital Instruments) with a nominal spring constant of 0.7 N/m were utilized.



**Suppl. Fig. 3:** (A) AFM image ( $3 \times 3 \mu\text{m}$ ;  $z = 3 \text{ nm}$ ) of SbpA protein recrystallization on gold surface. (B) Cyclic voltammetry of 5mM FCN in (i) the absence and (ii) presence 30 mg/mL HSA using SbpA-covered electrodes as well as current-potential traces (iii) of plain/ uncoated band electrodes in the presence of 30 mg/mL HSA. (C) Fluorescence images of SbpA-[anti SbpA\_IgG- anti IgG\_TRITC] affinity complex taken at increasing focal points from the bottom glass substrate, PDMS side walls and top PDMS microchannel.

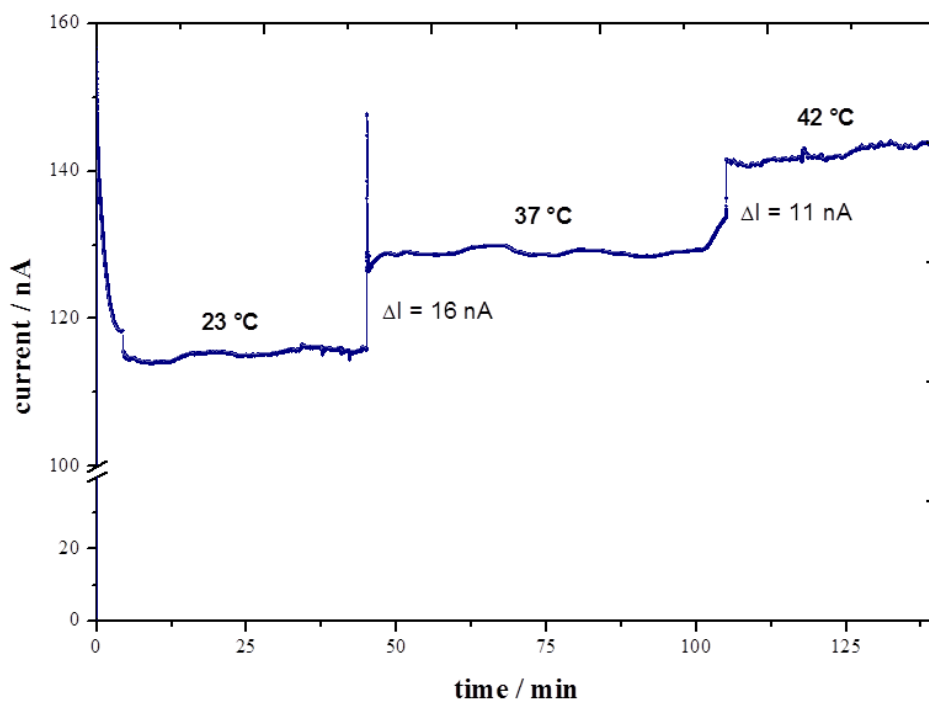
Fluorescence microscopy was used to evaluate the S-layer coating at the bottom, side and top walls of the microfluidic channels by adjusting the focus of the fluorescence microscope (Nikon Eclipse TE2000-S fluorescence microscope, Melville, NY). Following a

12 h recrystallization period, the SbpA was immunolabeled. Therefore the protein layer was incubated with 3% lactose blocking solution in PBS for 1 h. After removing the blocking solution, the protein layer was washed with PBS pH 7.2 for 20 min and incubated for 1 h using a 1:10 diluted serum solution containing anti-SbpA IgG (derived from rabbit). SbpA layer formation at the bottom, side and top walls of the microfluidic channels was detected after 1 h incubation with a second tetramethyl rhodamine isothiocyanate (TRITC) labeled antibody that binds to the rabbit IgG using a TRITC fluorescence filter (excitation at  $540 \pm 2$  nm; emission at  $605 \pm 55$  nm).

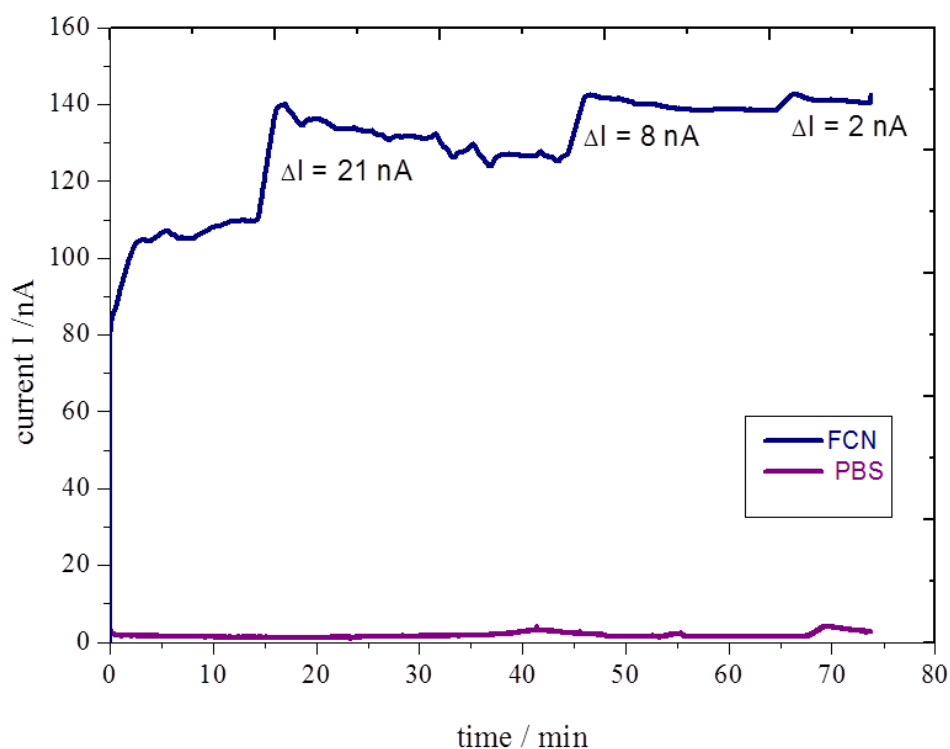


**Suppl. Fig. 4:** Schematic layout of the surface plasmon resonance (SPR) set up and SbpA recrystallization kinetics under flow conditions at  $100 \mu\text{L}/\text{min}$  using SPR measurements.

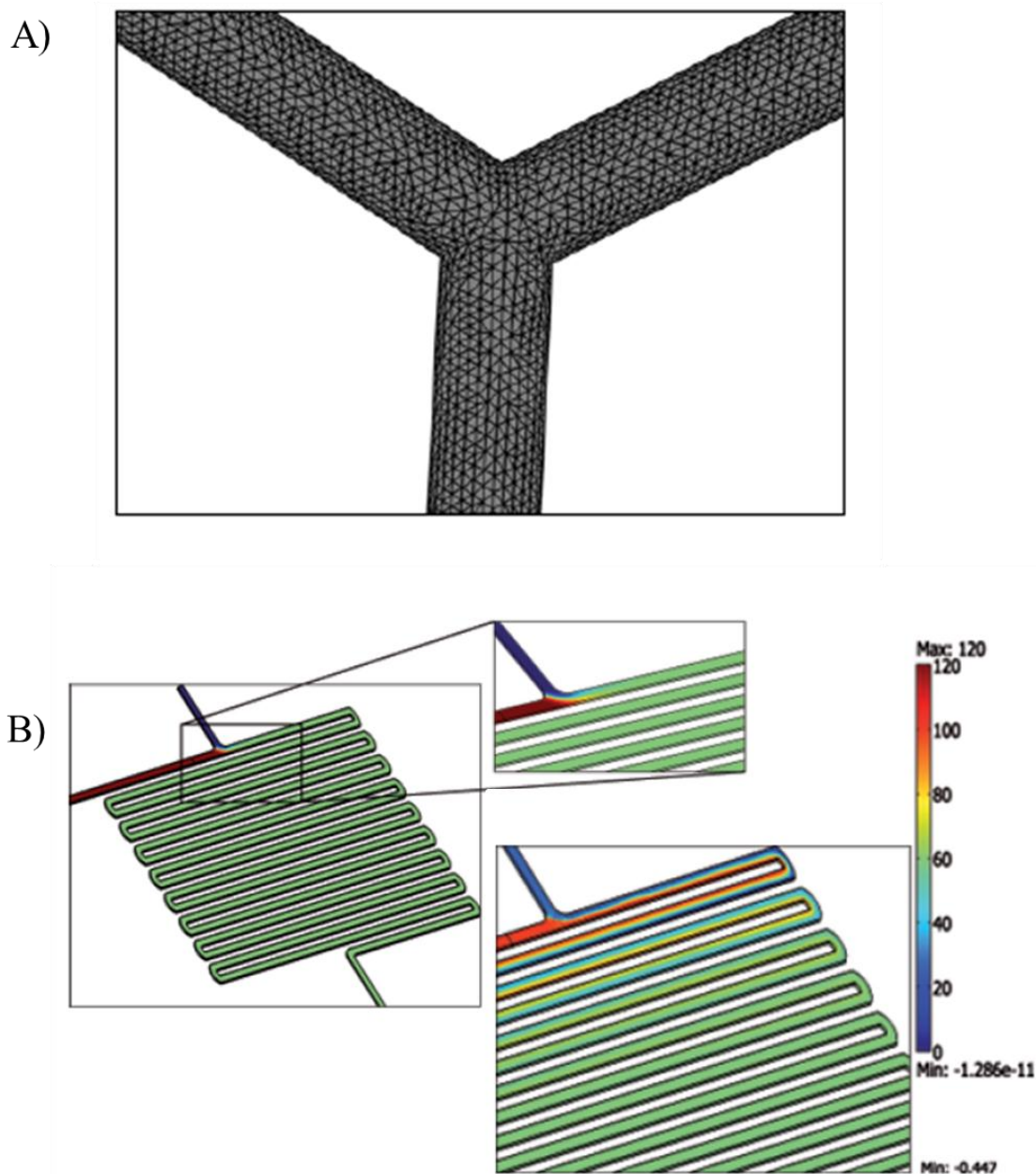
A)



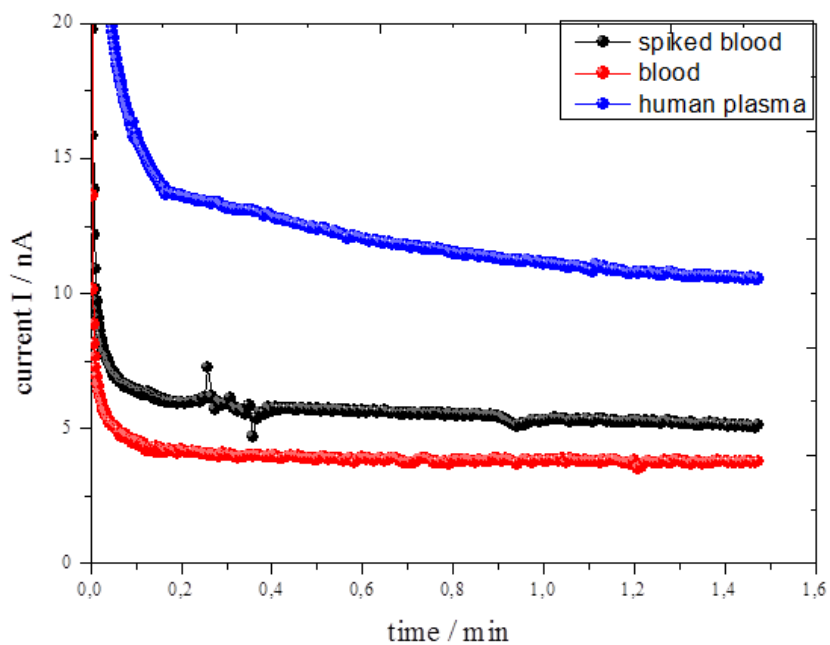
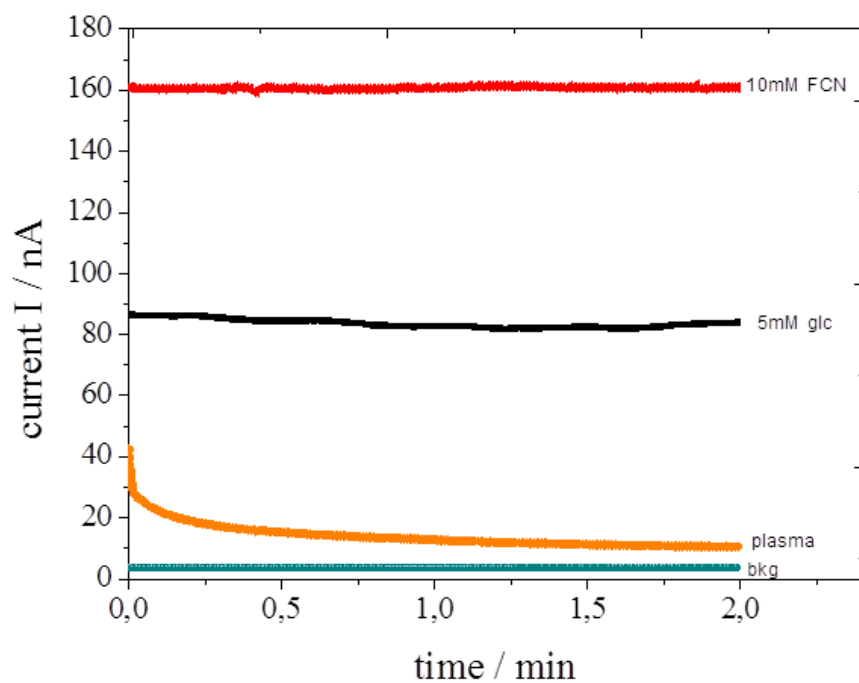
B)



**Suppl. Fig.5** (A) CV of 5mM FCN using the 3electrode configuration of MR1. (B) amperometric traces of 10mM FCN an PBS in the presence of increasing temperatures. (C) Amperometric currents of 10mM FCN in the presence of increasing flow velocities.

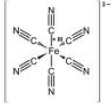
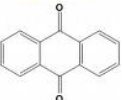
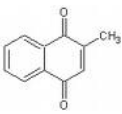


**Suppl. Fig. 6:** CFD simulations investigating convection and diffusion behavior following the introduction ferricyanide (inlet A) and GOx (inlet B) in a microreactor. A 3D computational fluid dynamics (CFD) simulation was conducted to determine local flow conditions and passive mixing behavior within the microreactor. The software COMSOL Multiphysics 3.4 containing the MEMS modules microfluidics/incompressible Navier-Stokes/convection and diffusion were used to calculate the optimum channel length of the microreactors. The final mesh consisted of approx. 4,700 000 hexahedral elements with an average side length of  $\sim 2.5 \mu\text{m}$  (see suppl. information, Fig. 5). The following parameters and boundary conditions were used to simulate flow profiles: laminar fluid flow, no-slip boundary conditions, constant inlet velocity ( $u$  of  $1 \times 10^{-4} \text{ m/s}$ ), zero pressure outlet, and a non-compressible Newtonian fluid with a dynamic viscosity ( $\eta$ ) of  $0.0051 \text{ Pa}\cdot\text{s}$  and density of ( $\rho$ )  $1.055 \times 10^3 \text{ kg/m}^3$ .



**Suppl. Fig 7.** : Amperometric measurements (2min) conducted in the four microreactors using 10mM FCN, 5mM glc, plasma and blood.

**Suppl. Table 1:** GOx activity after 24h storage in buffer and different mediator solutions at RT

Redox couple	Structure	Concentration	Solubility in PBS	Remaining* GOx activity	Signal to noise ratio
		mM	++/ +/ -	%	S/N
Hydroquinone/ quinone		1	++	90	80:1
Ferrocyanide/ ferricyanide		1	++	96	93:1
8-hydroxyquinoline		1	-	n.a.	n.a.
Anthraquinone/ anthrahydroquinone		1	+	79	2:1
Menadiol/ menadione		1	-	n.a.	n.a.

\* Amperometry performed in triplicate measurements

**Suppl. Table 2:** Amperometric signals of decreasing concentrations of mediator – enzyme mixtures following 10 min reaction time using a standard electrochemical cell.

FCN	GOx activity in nA		
	mM	100 µg/mL	50 µg/mL
100	1597	1299	422
70	1510	1272	468
<b>60</b>	<b>1433</b>	<b>1348</b>	<b>505</b>
50	1418	263	97
40	378	222	67
30	264	133	27
20	138	77	-
10	55	31	12
5	32	12	2
1	2	4	1

**Suppl. Table 3:** Comparison of mixing efficiency between integrated microfluidic serpentine reactor and commercially available external Tee-micromixer. Amperometric currents were recorded using the microfluidic three Pt band electrode set up.

Flow rate	External mixer	Microreactor	Capacity
mm/s	nA	nA	%
2	29.1	17.7	60.8
7	28.5	7.0	24.6
20	19.2	10.1	52.6